ELSEVIER

Journal of Alloys and Compounds 434–435 (2007) 809–812

Journal of ALLOYS AND COMPOUNDS

www.elsevier.com/locate/jallcom

Synthesis and characterisation of europium activated yttrium oxide fine powders

Elisabeth-Jeanne Popovici [a],*, Laura Muresan [a], Hristea Amalia [a],
Emil Indrea [b], Marilena Vasilescu [c]

[a] *"Raluca Ripan" Institute for Research in Chemistry, Fântânele 30, 400294 Cluj-Napoca, Romania*
[b] *National Institute for R&D for Isotopic and Molecular Technologies, Donath 71-103, 400293 Cluj-Napoca, Romania*
[c] *"I.G. Murgulescu" Institute of Physical Chemistry of the Romanian Academy, 202 Spl. Independentei, 060022 Bucureşti, Romania*

Abstract

In order to prepare fine powders of red emitting Y_2O_3:Eu phosphors, the reagent simultaneous addition (*SimAdd*) technique was developed and the influence of some preparative conditions on morpho-structural and optical properties of phosphors was studied. There was revealed that the precipitating reagent type and the pH of the precipitation medium influence on the photoluminescence (PL) properties as well as on the microstructure and morphology of phosphor particles. The *SimAdd*-technique enables us to prepare fine powders (<1 μm) of Y_2O_3:Eu phosphors with relatively good PL performances to be used in modern optoelectronic devices.

Keywords: Phosphors; Chemical synthesis; Scanning electron microscopy; Luminescence

1. Introduction

Europium activated yttrium oxide (Y_2O_3:Eu) is a well-known red emitting phosphor whose utilisation depends on luminescence performances and powder characteristics that are defined during the synthesis stages. Nowadays, there is a continuous demand for fine powders of efficient phosphors for modern optoelectronic devices [1–3]. Luminescence efficiency and colour purity, particle morphology or size and crystalline order degree are factors that determine the use of Y_2O_3:Eu based powders in plasma display panels (PDP's) or light emitting diodes (LED's). Usually, Y_2O_3:Eu phosphor is prepared by solid-state reaction (SSR) route that leads to microcrystalline (5–10 μm) powders with intense photoluminescence [4]. Alternative synthesis methods like wet-chemical and, particularly, sol–gel routes are used in order to obtain small phosphor particle sizes [5–11]. The goal of our studies is to synthesize, by wet-chemical synthesis route, fine powders of Y_2O_3:Eu phosphors with good luminescent performances. In this respect, *the reagent simultaneous addition technique* (*SimAdd*) was developed and the influence of some preparative conditions on morpho-structural and optical properties of Y_2O_3:Eu phosphors was studied.

2. Experimental part

Luminescent materials were prepared by the thermal treatment of precursors obtained from yttrium–europium (Y–Eu) nitrate mixture and ammonium oxalate, urea or ammonium carbonate as precipitating reagent (P.R.). The $0.97Y(NO_3)_3$–$0.03Eu(NO_3)_3$ mixture was prepared by dissolving Y_2O_3 and Eu_2O_3 (both 99.99%, Merck) in diluted nitric acid (Merck). Equal volumes of Y–Eu nitrate mixture (0.30 M) and P.R. solution (0.45–0.60 M) were simultaneously added into 1:10 diluted P.R. solution. Precipitation was carried out under continuous stirring and pH control. The post-precipitation stage consisted of 24 h aging, centrifuge separation, water wash and drying. The precursors thermal treatment was performed at 1100 °C, for 2 h, in air, without or with barium chloride additive to give the so-called no-flux phosphors or $BaCl_2$–phosphors, respectively. The as obtained material was water washed, dried and sieved; no ball milling was used.

Precursors and phosphors were characterised by *thermal analysis* (Paulik-Erdely Derivatograf OD-102; heating rate 6 °C/min), *infrared absorption spectroscopy* (JASCO 610 FTIR Spectrometer; KBr pellets technique), *photoluminescence measurements-PL* (Perkin-Elmer 204 Fluorescence Spectrophotometer; $\lambda_{exc} = 254$ nm), *X-ray diffraction-XRD* (DRON3M-Diffractometer; Co Kα radiation; Fe filter) and *scanning electronic microscopy-SEM* (JEOL-JSM 5510LV Microscope; Au-coated; secondary electron mode at an accelerating voltage of 20 kV). XRD data were processed in order to determine the crystalline

---

* Corresponding author.
E-mail address: jennypopovici@yahoo.com (E.-J. Popovici).

0925-8388/$ – see front matter © 2006 Elsevier B.V. All rights reserved.
doi:10.1016/j.jallcom.2006.08.312

Table 1
Precursor synthesis conditions (P.R. type, reagent ratio M:X, temperature, medium pH) and some characteristics of precursors (weight loss at 1100 °C, ΔW; thermal effect) and phosphors (PL intensity)

Precipitation conditions				Precursors				Phosphors	
P.R. type	M:X[a]	T (°C)	pH	Code	ΔW (%)	Thermal effect[b]	General composition	Code	PL (%)
$(NH_4)_2C_2O_4$	2:3	20	8.0[c]	PG5	54.5	Endo-220, 420 °C; exo-460, 620 °C	$Y_2(C_2O_4)_3 \cdot xY(OH)_3 \cdot yH_2O$	P5	59.3
$(NH_4)_2C_2O_4$	2:3	20	4.0[c]	PG7	54.0	Endo-220, 420 °C; exo-470, 660 °C	$Y_2(C_2O_4)_3 \cdot xY(OH)_3 \cdot yH_2O$	P7	84.3
$(NH_4)_2C_2O_4$	2:3	20	6.0[c]	PG8	60.0	Endo-220, 430 °C; exo-460, 660 °C	$Y_2(C_2O_4)_3 \cdot xY(OH)_3 \cdot yH_2O$	P8	63.1
$(NH_4)_2C_2O_4$	2:3	20	5.0[c]	PG9	59.0	Endo-250, 450 °C; exo-470, 620 °C	$Y_2(C_2O_4)_3 \cdot xY(OH)_3 \cdot yH_2O$	P9	62.7
$(NH_4)_2C_2O_4$	1:2	80	5.0	PG13	62.0	Endo-250, 420 °C; exo-510, 600 °C	$Y_2(C_2O_4)_3 \cdot xY(OH)_3 \cdot yH_2O$	P13	81.5
$(NH_2)_2CO$	1:2	80	5.7	PG14	40.8	Endo-195, 390, 620 °C	$Y(NO_3) \cdot xY(OH)_3 \cdot yH_2O$	P14	23.4
$(NH_4)_2CO_3$	1:2	80	5.2	PG15	45.5	Endo-310, 615 °C	$Y_2(CO_3)_3 \cdot xY(OH)_3 \cdot yH_2O$	P15	60.8

[a] Stoichiometric (2:3) and in excess (1:2) P.R. amounts.
[b] Characteristic thermal effects on DTA curves.
[c] Ammonia pH-correction.

structure and cell parameters (CrysFire method program) as well as the microcrystalline parameters (XRLINE program based on Warren-Averbach applied to band-profile).

3. Results and discussion

Objectives of this paper were to study the influence of the precipitating reagent (P.R.) on precursor and phosphors quality and to put in evidence the effect of the pH of the precipitation medium. In this respect, two precursors series were prepared namely PG13, PG14 and PG15 samples obtained with ammonium oxalate, urea and ammonium carbonate as P.R. and PG5, PG7, PG8, and PG9 samples obtained at different precipitation pH. Experimental conditions (harmonised to P.R. type) and some of precursor and phosphor characteristics are presented in Table 1. The mentioned precursor composition neglects the europium activator (~3 mol%) and the carbonate traces presents in almost all the samples. The PL intensity of the corresponding no-flux phosphors was determined from the emission spectra, in comparison with the SSR-standard (Y_2O_3:Eu, Kemira) considered 100%.

3.1. Influence of the precipitating reagent on precursors and phosphors quality

Precipitating reagent directly determines the precursor composition, as shown by their *thermal behaviour* and *FTIR spectra*. The thermal analysis curves possess typical features for basic oxalate (specific exo-effect!), basic nitrate and basic carbonate as formed with ammonium oxalate, urea and ammonium carbonate, respectively. The vibrational spectra of precursors consist of some characteristic bands, i.e. ν(H–O) ~ 3470, ν(C=O) ~ 1640, ν(C–O) ~ 1325, δ(O–C=O) + (Y–OH) ~ 814–790 for PG13; ν(H–O) ~ 3495, $\nu(NO_3)$ ~ 1384, ν(Y–O) ~ 638 for PG14 and ν(H–O) ~ 3422, $\nu(CO_3)$ ~ 1535, 1400, ν(Y–OH) ~ 838 cm^{-1} for PG15.

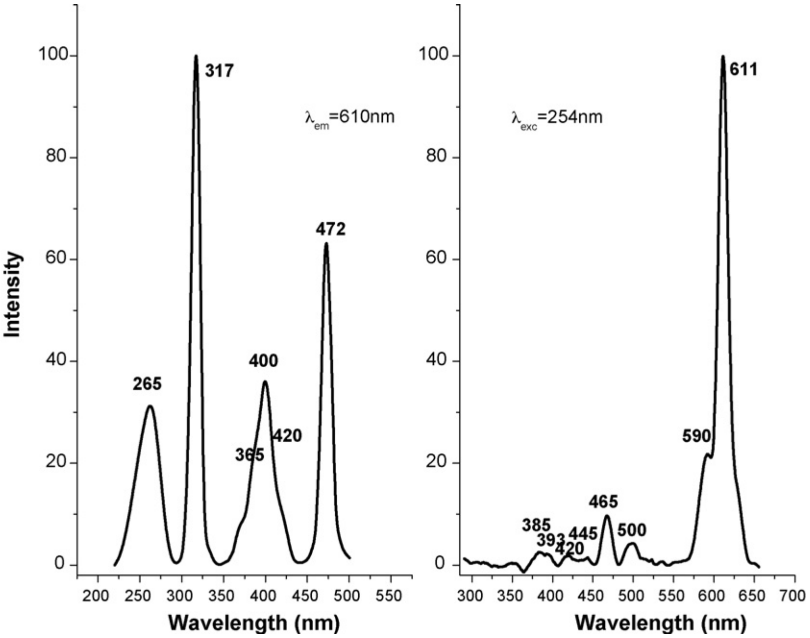

Fig. 1. Excitation (left) and emission (right) spectra of phosphor sample P13 (P.R. = $(NH_4)_2C_2O_4$).

The thermal treatment of precursors leads to their complete conversion into europium activated yttrium oxide samples, Y_2O_3:Eu or $Y_{2-x}Eu_xO_3$. *Photoluminescence* of red emitting Y_2O_3:Eu phosphor was evaluated on the basis of excitation and emission spectra (Fig. 1). Phosphors excitation proceeds mainly in the charge transfer band (Eu^{3+}–O^{2-}), in the UV domain. Under 254 nm excitation, the phosphor emits predominantly in the red domain, i.e. at ~590 nm ($^5D_0 \rightarrow {}^7F_1$electronic transition) and ~611 nm ($^5D_0 \rightarrow {}^7F_2$ transition). PL properties show that, in our thermal synthesis conditions, Y–Eu precursors are converted into Y_2O_3 crystalline lattice in which part of the Y^{3+} ions are substituted by Eu^{3+} species. The ionic radii (Eu^{3+} = 0.109 nm; Y^{3+} = 0.104 nm) as well as the precursor composition are favourable to the formation of the emission centres.

Photoluminescence intensity of phosphors strongly depends on the precipitating reagent (see Table 1). The best results are obtained with ammonium oxalate (P13, I = 81.5%) whereas the worst with urea (P14, I = 23.4%). One supposes that for urea, the low precipitation pH generates precursors with low PL ability. In fact, the correction of pH from ~5 to ~8 leads to a considerable PL improvement (49.1%).

Crystalline structure of phosphors is rather homogeneous, illustrating the Y_2O_3–Eu_2O_3 solid solution formation with no side or residual products (Fig. 2). Well-crystallized powders with cubic structure were formed, in agreement with the literature data (PDF 251011).

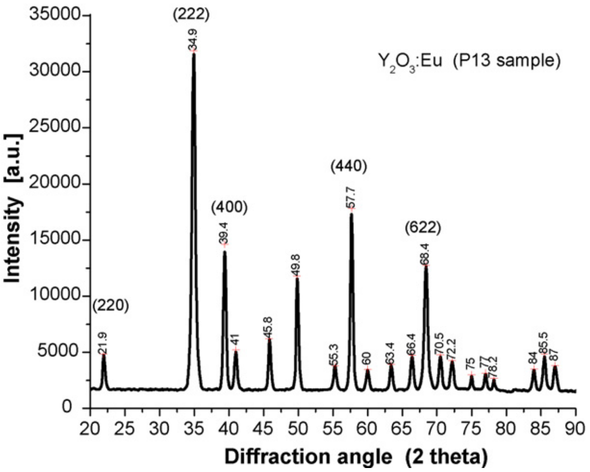

Fig. 2. XRD pattern of the no-flux phosphor prepared with ammonium oxalate as P.R.

The precipitating reagents could also influence the precursor and phosphor *morphology and particle size*, as illustrated by the SEM images (Fig. 3). Precursors consist of aggregates of crystals with different shape and sizes: 1–3 μm prismatic-lamellar (PG13), 0.2–0.3 μm spherical (PG14) and ~5 μm needle shaped (PG15). As for the corresponding no-flux phosphors, these ones preserve the original precursors shape, but they diminish in size with about 50%.

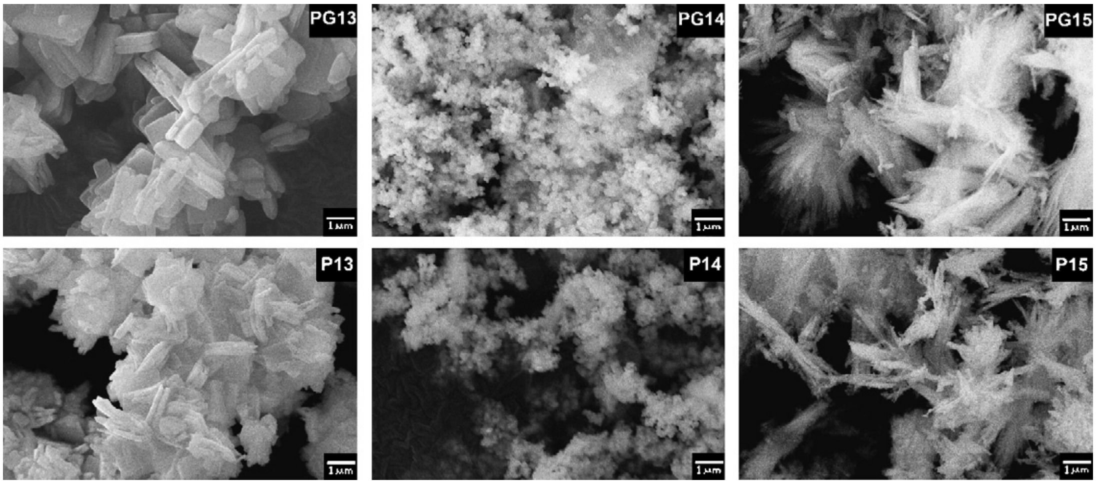

Fig. 3. SEM images of precursors prepared with ammonium oxalate (PG13), urea (PG14) and ammonium carbonate (PG15) and the corresponding no-flux phosphors (P13, P14, and P15).

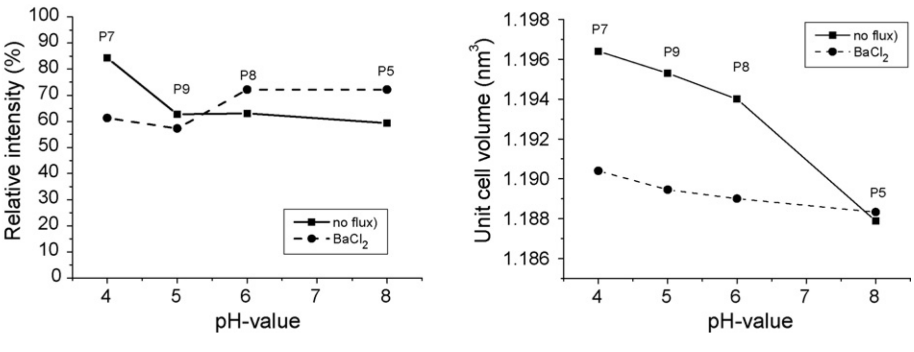

Fig. 4. Dependence of the PL relative intensity (left) and cell unit volume (right) on the precipitation pH of no-flux and $BaCl_2$–phosphors (V_{theor} = 1.1924 nm^3).

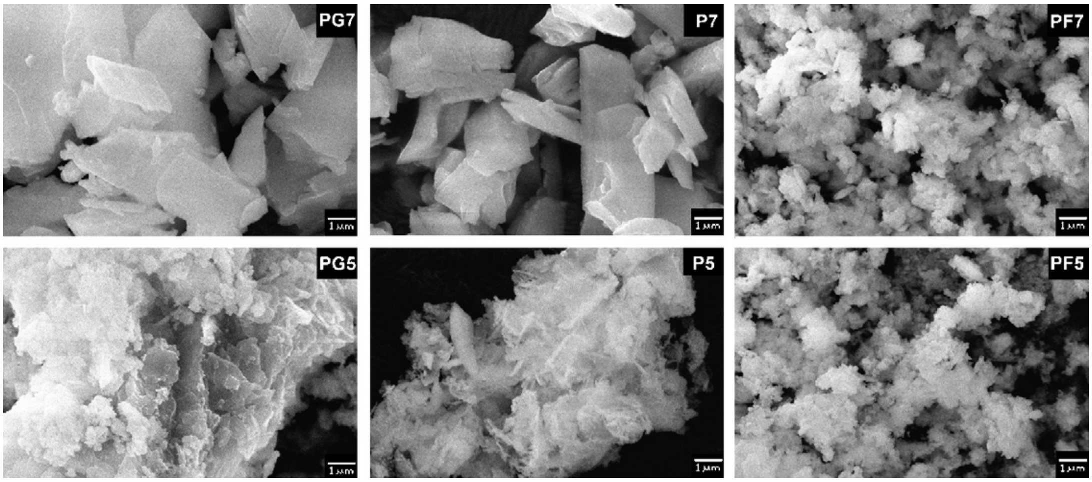

Fig. 5. SEM images of precursors and the corresponding no-flux phosphors and $BaCl_2$–phosphors obtained at pH ∼ 8 (PG7, P7, and PF7) and pH ∼ 4 (PG5, P5, and PF5).

3.2. Effect of the pH of the precipitation medium

Photoluminescence intensity and structural parameters of phosphors are influenced by the acidity of the precipitation medium (Fig. 4). For no-flux phosphors, the PL intensity decreases with the pH increasing, in parallel with the decrease of the unit cell parameters and volume ($V = 1.1964 \rightarrow 1.1879\,\text{nm}^3$). For $BaCl_2$–phosphors, the PL intensity increases with the pH, whereas the unit cell parameter/volume is slowly decreasing ($V = 1.1904 \rightarrow 1.1883\,\text{nm}^3$). Flux effect is observed only at pH higher than 6.

The XRD patterns show that all these phosphors possess *similar cubic crystalline arrangement* with variable crystallite dimensions (D_{eff}), depending on the precipitation pH. One can note that D_{eff} decreases with the pH increasing, namely, from 31 (P7; pH 4) to 24 nm (P5; pH 8) for no-flux phosphors and from 32 (PF7; pH 4) to 26 nm (PF5; pH 8) for $BaCl_2$–phosphors. The flux effect is also put in evidence. The precipitation pH also influences *the morphology and particle sizes of phosphors*, as illustrated by the SEM images (Fig. 5). Precursors consist of aggregates of crystals with different consistency, from isolated particle material (PG5) to compact one (PG7). As for the luminescent materials, the no-flux phosphors preserve the precursors appearance whereas $BaCl_2$–phosphors become much more dispersed (powders of about 0.3–0.5 μm).

4. Conclusions

The *SimAdd* technique is an alternative wet-chemical synthesis route for phosphor synthesis that has the advantage to facilitate the control of some of the preparative parameters. The study revealed that both the precipitating reagent type and the precipitation pH influence on the PL properties as well as on the microstructure and morphology of phosphor particles. The *SimAdd* technique enables us to prepare fine powders (<1 μm) of Y_2O_3:Eu phosphors with relatively good PL performances (intensity higher then 80% of the RSS–phosphor). Further experiments are to be performed in order to improve the PL characteristics and powder dispersion ability.

Acknowledgements

The work was financially supported by the Romanian R&D programs CNCSIS (grant 1303/2004) and Matnantech (contract 220/2004).

References

[1] R.P. Rao, Solid State Commun. 99 (1996) 439–443.
[2] M.H. Lee, S.G. Oh, S.C. Yi, D.S. Seo, J.P. Hong, C.O. Kim, Y.K. Yoo, J.S. Yoo, J. Electrochem. Soc. 147 (2000) 3139–3142.
[3] X. Jing, T. Ireland, G. Gibbons, D.J. Barber, J. Silver, A. Vecht, G. Fern, P. Trowga, D.G. Morton, J. Electrochem. Soc. 146 (1999) 4654–4658.
[4] M.N. Nazarov, J.H. Khang, D.Y. Jeon, E.J. Popovici, L. Muresan, B.S. Tsukerblat, Solid State Commun. 133 (2005) 183–186.
[5] A. Hristea, E.J. Popovici, L. Muresan, R. Grecu, E. Indrea, M. Voicescu, Studia Universitatis Babes Bolyai, Seria Physica XLIX (2004) 185–188.
[6] L. Muresan, E.J. Popovici, A. Hristea, M. Vasilescu, I. Silaghi-Dumitrescu, Studia Universitatis Babes Bolyai, Seria Physica XLIX (2004) 182–184.
[7] Y.D. Jiang, J.L. Wang, F. Zhang, H.G. Paris, C.J. Summers, J. Mater. Sci. 13 (1998) 2950–2955.
[8] M.J. Martinez-Rubio, T. Ireland, J. Silver, G. Fern, C. Gibbons, A. Vecht, Electrochem. Solid State Lett. 3 (2000) 446–449.
[9] D. Sordelet, M. Akinc, J. Colloid Int. Sci. 122 (1988) 47–59.
[10] B. Djuricic, D. Kolar, M. Memic, J. Eur. Ceram. Soc. 9 (1992) 75–82.
[11] R.P. Rao, J. Electrochem. Soc. 143 (1996) 189–197.